

Application of Fullwaveform Tomography to VSP Walkaway Data

Eric Takam Takougang*
*Petroleum Institute
P.O. Box: 2533, Abu Dhabi
etakougang@pi.ac.ae*

Youcef Bouzidi
*Petroleum Institute
P.O. Box: 2533, Abu Dhabi
ybouzidi@pi.ac.ae*

SUMMARY

VSP walkaway data were collected in an oil field in the United Arab Emirates. 2D frequency domain fullwaveform tomography was used to obtain high resolution rock properties (P-wave), and structural information near and away from the borehole, following a specific data preconditioning and inversion strategy. The field data were inverted between 4 and 50 Hz, and the starting model was obtained from traveltimes tomography. The results of the inversion show zones with anomalous low velocities that correlate in places with known presence of hydrocarbons, and highlight their possible extensions. A comparison of the results at the borehole location with the sonic log shows a generally good match. However, some mismatches are evident and can be explained by possible anisotropy and out of the plane structures not taken into account during the inversion.

Key words: waveform tomography, traveltimes tomography, VSP walkaway

INTRODUCTION

Fullwaveform tomography is a qualitative and quantitative imaging technique that can provide high resolution velocity, attenuation, and density images of the subsurface, based on the seismic waveform. The algorithm is based on iteratively updating a starting velocity, density and/or attenuation model by minimising the difference between the field data and the modelled data obtained after forward modelling using the current velocity, density and/or attenuation models. Unlike other imaging techniques such as traveltimes tomography that uses only the first arrival traveltimes, fullwaveform tomography has the potential to use all the information contained in the seismic waveform (amplitude and phase), and thus provides an image with more details and greater resolution, depending on the frequency used in the inversion process (e.g. Pratt et al., 1999, Malinowski et al., 2011, Takam Takougang and Calvert, 2013). However, fullwaveform tomography is a highly non-linear process, a consequence of the abundance of information included during the inversion. To mitigate the non-linearity of fullwaveform tomography, it is necessary to adopt a good preconditioning and inversion strategy (e.g. Takam Takougang and Calvert, 2013; Kamei et al., 2014; Brenders and Pratt, 2007). Due to the limiting computational power and the complexity of the forward solver, most of the applications in this domain are in 2D rather than 3D, and acoustic or visco-acoustic rather than visco-elastic; although recent applications with 3D elastic algorithms were reported in the literature (e.g. Lee et al., 2014). Several successful applications of fullwaveform tomography ranging from crustal studies using wide angle refraction data to reflection seismic can be found in the literature (e.g., Takam Takougang and Calvert, 2011, Malinowski et al., 2011; Kamei et al., 2014). A few applications with cross-hole data can also be found in the literature (e.g. Wang and Rao, 2006; Pratt et al., 2003), but rarely with VSP walkaway data (e.g. Gao et al., 2011), perhaps due to the non-availability of datasets.

In this paper, we present an application of fullwaveform tomography to VSP walkaway data from an oil field. Our goal is to provide images of greater resolution in the borehole and away from the borehole that will enable a better understanding of the subsurface rock properties. We present the pre-processing steps and inversion strategy that resulted in successfully building a P-wave velocity model that correlates well with the available sonic log.

APPLICATION TO VSP WALKAWAY DATA

Multi-offset Vertical Seismic Profile (VSP walkaway) data were collected in an oil field located in a shallow water environment, offshore the United Arab Emirates. The purpose of the survey was to provide structural information of the reservoir, around and away from the borehole. A typical air gun was used to shoot five lines at 4 m source depth. Each line was shot twice in both directions (left and right) making a shot interval of 25 m. A typical recording tool with 20 receivers spaced every 15.1 m was used. Each line was recorded with a variable maximum offset, depending on the depth of the receivers. Smaller offsets were used for shallow receivers and larger offsets for deeper receivers. The selected 5 parallel lines (Line1, Line2, Line3, Line4, and Line5) were merged to form the input dataset for waveform tomography. Line1 has 20 receivers located at shallow depths while Line2, 3, 4 and 5 have receivers located at mid to deeper depths. The recording tool was located in the borehole, deviated with an angle varying between 0 and 24 degree from the vertical direction. The total length of the combined lines was 9 km, containing 1344 shots and 100 receivers located half way down the borehole. It is worth mentioning that this unusual geometry is not ideal for fullwaveform tomography, as only 20 receivers were used for each shot, and the depths between receiver groups were irregular, creating gaps in the ray coverage, especially between the shallow and mid receiver groups.

Data preconditioning and inversion

A successful application of waveform tomography requires a robust inversion strategy to avoid cycle skipping, and ensure adequate convergence to the global minimum. A good preconditioning of the data is also necessary. We used the frequency domain acoustic waveform tomography algorithm as described in Pratt (1999). For the acoustic waveform inversion, the preconditioning of the data is necessary to ensure that they can be predicted by the acoustic wave-equation. Figure 1 shows a receiver gather at shallow depth; the presence of what is believed to be converted shear waves (indicated by the blue arrow in Figure 1), probably due to mode conversion at the water-seabed interface can only be predicted by the elastic wave-equation, and need to be removed for the acoustic waveform inversion. The data were muted with a maximum time window of 164 ms after the first arrival to avoid the inclusion of these

converted shear waves as well as late multiples. The amplitudes of the data were corrected from 3D to 2D propagation by multiplying the data by \sqrt{t} (t is the propagation time), and traces contaminated by noise were removed. Traveltime tomography (Aldridge and Oldenburg, 1993) was used to generate the starting model from the first arrival traveltimes. We adopted a multiscale waveform tomography approach consisting of inverting from the minimum frequency to the highest frequency, and increasing the time window of the data progressively with increasing frequencies. The inversion was performed with frequencies ranging from 4 Hz to 40 Hz and 3 sets of time windows were used: 90ms after the first arrival traveltimes for frequencies 4-10 Hz, 120 ms after the first arrival traveltimes for frequencies 10-25 Hz, and 164 ms after the first arrival traveltimes for frequencies 25-40 Hz. The source signature was inverted following the method of Pratt (1999). Groups of 5 frequencies with a frequency interval of 0.5 Hz were inverted at a time, and the source signature was re-estimated after the inversion of each group of frequencies. 5 to 6 iterations were used per frequency group. The starting frequency (4 Hz) was chosen such that the starting model predicted the first arrival traveltimes to within half a cycle (Sirgue, 2003). It was not possible to select lower starting frequencies due to the increasing presence of noise with lower frequencies.

We noticed that the inclusion of amplitudes during the inversion resulted in the appearance of artefacts along the receiver locations in the borehole. As a consequence, only the phase was used during the inversion and the logarithmic

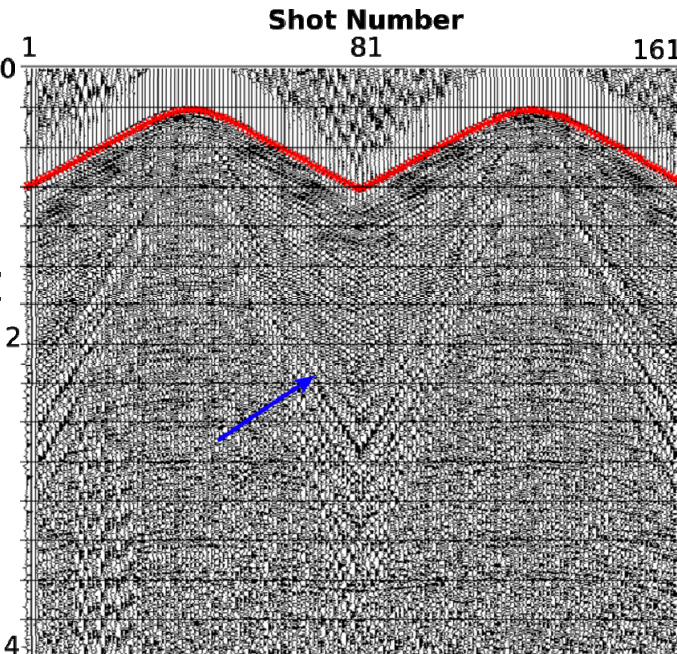


Figure 1: Common receiver gather at shallow depth. The blue arrow represents the presence of shear waves. First arrival traveltimes are indicated in red. An AGC operator length of 500 ms was used to display the data.

data residual was adopted. The logarithmic data residual had proven to provide results of comparable resolution to the logarithmic amplitude and phase residual of early arrival waveform inversion (Bednar et al., 2007; Shin et al., 2007; Kamei et al., 2014).

RESULTS AND DISCUSSION

The starting model and the result of the inversion are displayed in Figure 2. Fullwaveform tomography has provided an image of higher resolution than the starting model obtained from traveltimes tomography. The low velocity zone at $x = -500$ to $+500$ m and between depths z_4 and z_5 correspond to the location of known hydrocarbon reservoirs. The result clearly shows the extent of the reservoirs with great detail. A comparison of the 1D velocity profile along the borehole location and the P-wave velocity from the sonic log shows an overall good match (Figure 3). However, some mismatches are evident at certain locations which can be explained by the poor ray coverage at z_2 where there is an absence of receivers, the possible presence of anisotropy, and out of plane structures which were not considered during the inversion. We have merged five independent lines that were parallel but not co-linear to form the line for waveform tomography, and the well was deviated away from the plane defined by the lines. As such, further work will be considered to use a more appropriate 2.5D modelling to include out-of-plane structures which were ignored in this study.

CONCLUSIONS

2D frequency domain acoustic waveform tomography was applied to a VSP walkaway dataset from an oil field in the United Arab Emirates. 5 parallel lines were merged to form a line of 9 km in length with 1344 shots at 25 m shot intervals, and 100 receivers in a deviated borehole. Each line was recorded using a typical recording tool with 20 receivers and 15.1 m receivers' interval. The recording tool was deployed in a deviated well at different depths for each line. The result of the inversion shows a generally good match with the sonic log. Mismatches are present at certain locations which are certainly due to the lack of receivers at shallow to mid depths, possible presence of anisotropy, and out of plane structures ignored during the current inversion. The result shows low velocity zones that correlates with known locations of hydrocarbons.

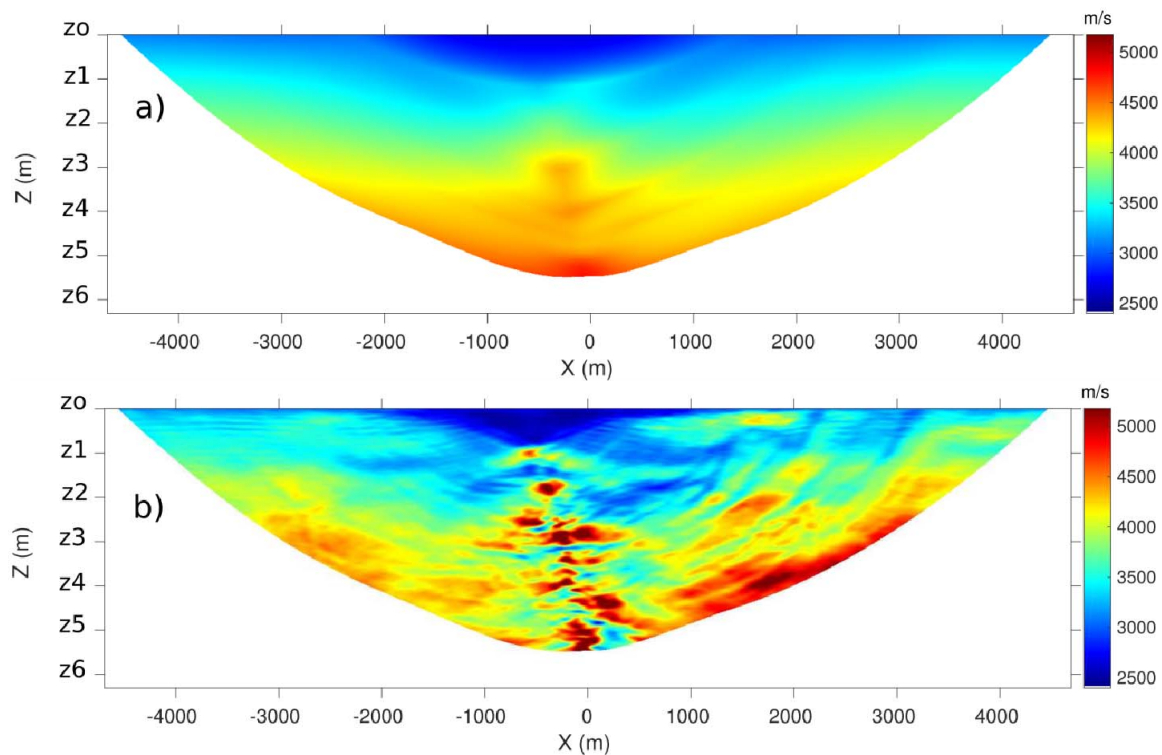


Figure 2: (a) Starting model from traveltim tomography; (b) Waveform tomography after 4-40 Hz inversion.

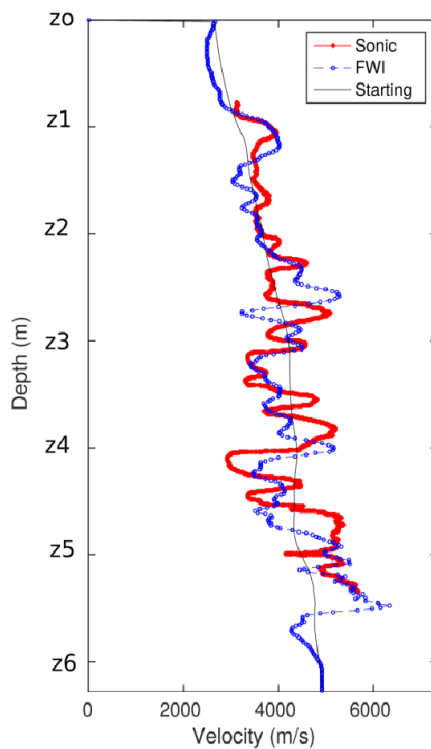


Figure 3: 1D velocity profile at the wellbore location. There is a generally good fit between the waveform tomography model (FWI) and the P-wave velocity from the sonic log (Sonic), with a significant improvement of the starting model (Starting).

ACKNOWLEDGMENTS

We are grateful to the Oil-Subcommittee of the Abu-Dhabi National Oil Company (ADNOC) and its operating companies (OPCOs) for sponsoring this project and providing the data. Special thanks to Marc Michel Durandeu and to all the committee members for their inputs and encouragements to the project. The waveform tomography code was provided by Gerhard Pratt.

REFERENCES

- Aldridge, D.F., and Oldenburg, D., 1993, Two-dimensional tomographic inversion with finite-difference traveltimes: *Journal of Seismic Exploration*, 2, 257–274.
- Bednar, J.B., Shin, C., and Pyun, S., 2007, Comparison of waveform inversion, part 2: phase approach: *Geophysical Prospecting*, 55, 465–475.
- Brenders, A. J., and Pratt, R.G., 2007, Full waveform inversion tomography for lithospheric imaging: results from a blind test in a realistic crustal model: *Geophysical Journal International*, 168, 133–151.
- Gao, F., Levander, A.R., Pratt, G., Zelt, C. A., and Fradelizio, G. L., 2006, Waveform tomography at a ground contamination site: VSP-surface data set: *Geophysics*, 71, H1-H11.
- Kamei, R., Pratt, R.G., and Tsuji, T., 2014, Misfit functionals in Laplace-Fourier domain waveform inversion, with application to wide-angle ocean bottom seismograph data: *Geophysical Prospecting*, 62, 1054–1074.
- Lee E.J., Po Chen, Jordan, T.H., Maechling, P.B., Denolle, M.A.M., and Beroza, G.C., 2014, Full-3-D tomography for crustal structure in Southern California based on the scattering-integral and the adjoint-wavefield methods: *Journal of Geophysical Research: Solid Earth*, 119,6421-6451.
- Malinowski, M., Operto, S., and Ribodetti, A., 2011, High-resolution seismic attenuation imaging from wide-aperture onshore data by visco-acoustic frequency-domain full-waveform inversion: *Geophysical Journal International*, 186, 1179–1204.
- Mao W., and Stuart, G.W., 1997, Transmission-reflection tomography: Application to reverse VSP: *Geophysics*, 62, 884-894.
- Pratt, R.G., 1999, Seismic waveform inversion in the frequency domain, Part 1: Theory and verification in a physical scale model: *Geophysics*, 64, 888–901.
- Pratt, R.G., Bauer, K., and Weber, M., 2003, Crosshole waveform tomography velocity and attenuation images of arctic gas hydrates: *SEG Technical Program Expanded Abstracts*, 573, 2255-2258.
- Sirgue, L., 2003, Inversion de la forme d'onde dans le domaine fréquentiel de données sismiques grands offsets: Ph.D. thesis, École Normale Supérieure de Paris.
- Shin C., Pyun S., and Bednar J.B., 2007, Comparison of waveform inversion, Part 1: conventional wavefield vs logarithmic wavefield: *Geophysical Prospecting*, 55, 449–464.
- Takam Takougang, E.M., and Calvert, A.J., 2011, Seismic waveform tomography across the Seattle Fault Zone in Puget Sound: resolution analysis and effectiveness of visco-acoustic inversion of viscoelastic data: *Geophysical Journal International*, 193,763-787.
- Wang, Y., and Rao, Y., 2006, Crosshole seismic waveform tomography -1. Strategy for real data application: *Geophysical Journal International*, 166, 1224–1236.